IEEE Std 1302-1998

# IEEE Guide for the Electromagnetic Characterization of Conductive Gaskets in the Frequency Range of DC to 18 GHz

## IEEE Electromagnetic Compatibility Society

Sponsored by the
Standards Committee

26 June 1998 SH94613

# IEEE Guide for the Electromagnetic Characterization of Conductive Gaskets in the Frequency Range of DC to 18 GHz

Sponsor

**Standards Committee**
**of the**
**IEEE Electromagnetic Compatibility Society**

Approved 20 May 1998

**IEEE-SA Standards Board**

**Abstract:** Information to assist users of gaskets in evaluating gasket measurement techniques to determine which reveal the properties critical to the intended application, to highlight limitations and sources of error of the competing measurement techniques, and to provide a basis for comparing the techniques is provided. Emphasis is placed on those measurement techniques that have been adopted through incorporation into standards, both commercial and military, or that have been used extensively.
**Keywords:** aperture transmission, electromagnetic interference (EMI) gaskets, electromagnetic shielding, measurement techniques, reverberation chamber, stirred mode, transfer impedance

---

The Institute of Electrical and Electronics Engineers, Inc.
345 East 47th Street, New York, NY 10017-2394, USA



ISBN 0-7381-0183-4

# Introduction

(This introduction is not part of IEEE Std 1302-1998, IEEE Guide for the Electromagnetic Characterization of Conductive Gaskets in the Frequency Range of DC to 18 GHz.)

An electromagnetic interference (EMI) gasket is a conductive material that is used to improve the electrical bonding between metallic parts of an electronic chassis, equipment enclosure, or electromagnetic shield. A wide variety of materials and techniques are used to produce EMI gaskets. The effectiveness of gaskets in the closing of seams and joints is dependent upon the properties of the gasket and the method of installation. Several techniques are available to measure the electromagnetic properties of EMI gaskets. Unfortunately, measurement results are often inconsistent between techniques.

This document provides guidance on the use of recognized techniques for the electromagnetic performance characterization of EMI gaskets. It does not recommend one technique over another. It is recognized that some or all of the "alternative" techniques may, at some time in the future, become widely accepted and practiced. At that time, this guide will be revised to reflect their adoption. It is also recognized that efforts are currently underway to revise the measurement techniques currently covered in this guide. These revisions will be included in future updates of this guide.

The theory of gasket behavior given in this guide is highly simplified, and is intended to illustrate primary principles only. For a greater understanding of the electromagnetic interactions that occur in a gasketed joint, the reader is advised to consult the many excellent mathematical treatments in books and papers available through the IEEE and other technical publishers.

## Participants

The following persons were members of the P1302 Working Group and contributed to the preparation of this guide:

**Hugh W. Denny,** *Chair*

Dale Ashby
Dwayne R. Awerkamp
Robert Benn
Ronald W. Brewer
Joseph E. Butler, Jr.
David Castro
Hafeez Choudhary
Gary Fenical
Richard T. Ford
Gustav J. Freyer
Bob Gibson
Mark Hansen
Michael O. Hatfield
William Hoge
Robert Johnk
D. Mark Johnson
Galen Koepke
George M. Kunkel
Phillip Lessner
Michael McInerney
Bob Mulhall
Steve Mullenix
W. Drew Peregrim
John P. Quine
T. J. Ritenour
Robert A. Rothenberg
Joseph Rowan
Michael Taylor
David A. Weston

The following persons were on the balloting committee:

Dale Ashby
Dwayne R. Awerkamp
Stephen H. Berger
Ronald W. Brewer
Edwin L. Bronaugh
Joseph E. Butler, Jr.
Hugh W. Denny
Franz Gisin
David A. Graham
Donald N. Heirman
Lothar O. Hoeft
Daniel D. Hoolihan
Motohisa Kanda
John G. Kraemer
George M. Kunkel
William McGinnis
Michael K. McInerney
Dheena Moongilan
Robert Mulhall
John D. Osburn
Jose Perini
John P. Quine
T. J. Ritenour
Robert A. Rothenberg
Joseph Rowan
Risaburo Sato
Michael J. Scougall
Ralph M. Showers
Ronald T. Stickney
Dale Svetanoff
Donald L. Sweeney
David L. Traver
David A. Weston

The final conditions for approval of this standard were met on 20 May 1998. This standard was conditionally approved by the IEEE Standards Board on 19 March 1998, with the following membership:



 

# Contents

# IEEE Guide for the Electromagnetic Characterization of Conductive Gaskets in the Frequency Range of DC to 18 GHz

## 1. Overview

### 1.1 Background

The ideal electromagnetic shield is an infinitely conductive enclosure with no apertures or penetrations of any kind. The functional requirements and practicalities of design and construction, however, prevent this ideal from being realized. Penetrations for power, signals, and ventilation must be provided. Access apertures for calibrations, controls, and adjustments must exist. The different pieces of chassis and enclosure must be joined for the final product.

Electromagnetic energy exits or enters the shield at apertures, along conductive penetrations, and through imperfect seams. To restrict this coupling of energy to levels that are sufficiently low to comply with regulations and to permit interference-free operation, these unwanted coupling paths must be closed. Filters are used on the penetrations; screens and covers may be used over the apertures. Seams and joints, however, require special attention. For shielding, metal-flow processes such as welding, brazing, and soldering are the preferred methods for making joints and seams. Many situations arise, however, in which these techniques cannot be used, and in which direct metal-to-metal contact does not provide an adequate electromagnetic seal. In these cases, an electromagnetic interference (EMI) gasket must be installed in the joint.

EMI gaskets are conductive materials that are designed to conform to joint surfaces and to provide a low-impedance path. EMI gaskets are made from a wide variety of materials, such as beryllium copper, galvanized steel, stainless steel, electroplated steel, aluminum, and conductively loaded polymers. Conductor types include spring fingers, spiraled bands, perforated sheets, knitted wire mesh, conductive fabric, reinforced foil, and oriented wires. Materials added to polymeric binders to achieve conductivity include copper, silver, carbon, aluminum, and nickel as flakes, powders, wires, and coated spheres. The shapes available include sheets, strips, washers, tubes, and customized geometries.

The term “EMI gasket” is consistent with the generic industrial definition of a gasket. The electromagnetic fields that are being shielded impinge upon the conductive materials of the enclosure. The incident field induces currents in the enclosure walls. Seams represent discontinuities in shield current paths, with resulting voltage differentials across the seams. The purpose of the EMI gasket is to reduce the voltage differential across the seam because the strength of the field emanating from the seam is directly proportional to this voltage.

Depending upon function and application, electronic equipment must operate in an extremely wide range, in both intensity and frequency, of electromagnetic environments. The environments can vary from that of the home to that of the battlefield. Since there is no “one size/type fits all” gasket, the challenge that faces equipment designers is that of choosing the most cost-effective gasket for their particular application.

An essential parameter in this selection process is the degree to which the gasket prevents the electromagnetic energy that impinges on one side of the metal joint containing the gasket from coupling through the joint to the other side (i.e., the gasket’s electromagnetic sealing capability). Many factors determine the electromagnetic seal provided by an EMI gasket, including

a) The gasket material
b) The gasket construction
c) The geometry of the joint
d) The condition of the contact surfaces
e) The method of fastening
f) The closure pressure
g) The nature of the impinging field

The ideal EMI gasket measurement technique would reveal the full range of effects caused by mounting surface variations, aging, and fasteners, and would provide results that indicate the behavior that is expected from the gasket as installed. Currently, no single measurement technique does this over the frequency range of dc to 18 GHz.

### 1.2 Scope

This guide provides guidance on the selection of the best technique for measuring EMI gaskets for particular applications, identifies limitations and sources of errors of the commonly accepted techniques for measuring gaskets, and provides a basis for comparing the various accepted techniques. It encompasses measurements of the as-installed behavior of gaskets as well as manufacturing related, quality-control measurements.

### 1.3 Purpose

The purpose of this guide is to provide information that will allow the user of conductive gaskets to select the best measurement technique for a given application and to correctly interpret the data that is provided by each technique.

## 2. References

This guide shall be used in conjunction with the following standards. A bibliography is included in Clause 10 for further information.

ANSI/NCSL Z540-1-1994, Calibration—Calibration Laboratories and Measuring and Test Equipment—General Requirements.[1]

[1]ANSI publications are available from the Sales Department, American National Standards Institute, 11 West 42nd Street, 13th Floor, New York, NY 10036, USA.

 

ARP 1173-1988 (Reaff 1991), Test Procedure to Measure the RF Shielding Characteristics of EMI Gaskets.[2]

ARP 1705-1981 (Reaff 1991), Coaxial Test Procedure to Measure the RF Shielding Characteristics of EMI Gasket Materials.

ASTM D4935-89 (1994), Standard Test Method for Measuring the Electromagnetic Shielding Effectiveness of Planar Materials.[3]

Def Stan 59-103 (17-Sep-93), EMI/EMP Gasket Components.[4]

IEEE Std 100-1996, IEEE Standard Dictionary of Electrical and Electronics Terms.[5]

IEEE Std 299-1997, IEEE Standard for Measuring the Effectiveness of Electromagnetic Shielding Enclosures.

MIL-G-83528B (1993), General Specifications for Gasketing Material, Conductive, Shielding Gasket, Electronic, Elastomer, EMI/RFI.[6]

NCSL RP-12 (4/95), Recommended Practice for Determination and Reporting of Measurement Uncertainties.[7]

# 3. Definitions, acronyms, and abbreviations

## 3.1 Definitions

All terms used in this document are in accordance with IEEE Std 100-1996.

## 3.2 Acronyms and abbreviations

| | |
|---|---|
| ARP | aerospace recommended practice |
| dBμV/m | decibels above a microvolt per meter |
| dBμA/m | decibels above a microampere per meter |
| EME | electromagnetic environments |
| EMI | electromagnetic interference |
| MSC | mode-stirred chamber |
| SAE | Society of Automotive Engineers |
| SE | shielding effectiveness |
| TEM | transverse electromagnetic |

[2]Aerospace Recommended Practices are available from the Society of Automotive Engineers, 400 Commonwealth Drive, Warrendale, PA 15096, USA.

[3]ASTM publications are available from the American Society for Testing and Materials, 100 Barr Harbor Drive, West Conshohocken, PA 19428-2959, USA.

[4]Defence Standards may be obtained from the Ministry of Defence, Directorate of Standardization, Kentigern House, 65 Brown Street, Glasgow, Scotland, G2 8EX.

[5]IEEE publications are available from the Institute of Electrical and Electronics Engineers, 445 Hoes Lane, P.O. Box 1331, Piscataway, NJ 08855-1331, USA.

[6]MIL publications are available from Customer Service, Defense Printing Service, 700 Robbins Ave., Bldg. 4D, Philadelphia, PA 19111-5094, USA.

[7]NCSL publications can be obtained from the National Conference of Standards Laboratories, 1800 30th Street, Suite 305B, Boulder, CO 80301-1032, USA.

## 4. Factors affecting gasket performance

Figure 1 illustrates a typical application in which the EMI gasket is placed underneath the lip of a cover in order to close the gap between it and the base enclosure. Other similar applications are under connector shells, waveguide flanges, filter cans and meter flanges, and in seams. The objective of the gasket is to provide an electrical path across the gap in the shield, such that the impedance of the path through the gasket approaches that of a comparable span of the base shield. The impedance of the gasket is a function of its materials and construction, its geometry, and the interface between the gasket and the shield.

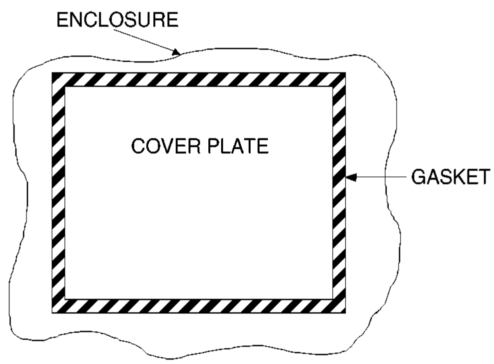


**Figure 1—Typical gasket application**

All gasket materials have resistive, inductive, and capacitive properties that may exhibit themselves over different portions of the frequency band. Which property determines the gasket's predominant characteristic depends upon the materials and construction of the gasket, as well as the geometry of the joint. Most gaskets can be considered resistive at low frequencies. Those gaskets that are constructed of metal filaments (oriented wires or wire meshes) and fingers or spirals typically appear as an inductance in series with a resistance. Gaskets that are formed from conductively loaded polymers typically appear as a shunt capacitance in parallel with a resistance. These complex impedances determine the effectiveness of the gaskets as frequency increases. Therefore, reliance on volume resistivity data taken at dc or at power frequencies can be very misleading.

All gaskets behave as complex networks of resistors, inductors, and capacitors at frequencies at which their physical dimensions become significant fractions of a wavelength, or the spacings between constituent elements approach or exceed resonant dimensions. Furthermore, the gasketed joint is polarized. This polarization is the consequence of the joint being long and narrow, and of the conductors of the gasket being preferentially aligned with a field component of the incident wave.

The gasketed joint can behave like a section of waveguide that is filled with conductive materials. When this happens, the gasket and aperture will exhibit complex radiation and transmission properties. Coupling through this aperture is likely to be of greater importance to shielding effectiveness than the enclosure itself. Where the gasket does not appear homogeneous, it is not safe to assume that the current through the gasket is uniform or that it is determined by the shield. The characteristics of the incident field must also be considered; the radiation characteristics of the total aperture must be recognized; and the propagation of the coupled wave through the "loaded" aperture must be taken into account.

Shield current encounters both the contact impedance between the gasket and the impedance of the gasket itself. On the contact surfaces, there are often films of metal oxides and sulfides, paints, cleaners, dust, dirt and environmental deposits. Such films will likely be present on gasket surfaces as well.

NOTE—Many surface films are nonconductive. Depending upon the compression-deflection properties of the gasket material, the nature of its conductive elements (e.g., “gritty” particles, oriented wires, knitted wires, etc.), and the closure force applied, certain gaskets will “bite” through such films more effectively than others. This “biting” may or may not be desirable, depending upon the application environment, as it may open a site for corrosion or galvanic action over the life of the equipment. Environmental testing should be considered for every application.

The path for current from the shield to the gasket will be through the ridges and valleys on the mating surface that result from machining or casting imperfections to the contacted portions of the gasket materials. The contact impedance between the gasket and the parent shield can be a significant factor in the overall behavior of the gasket. This contact impedance will have reactive components in addition to resistance. For example, there is usually some capacitive coupling between the contact surface and the conductors in the gasket.

In addition to the impedance of the gasket and the gasket-to-shield interface, the shield current encounters the resistive and inductive elements of the shield itself, and a portion flows around the gasket via the stray capacitance between the two pieces of parent material. Thus, the current path through a gasket is a complex network, as illustrated in Figure 2. As complex as this network appears, it is actually somewhat of a simplification. At very short wavelengths, in particular, the gasketed joint will also behave in roughly the same manner as the braid of a coaxial shield. The openings in the braid permit energy to leak through. Depending upon the specific configuration of the conducting elements of the gasket, these openings can render the gasket practically transparent at particular frequencies or over certain frequency ranges, see Quine, et al. [B20].[8]

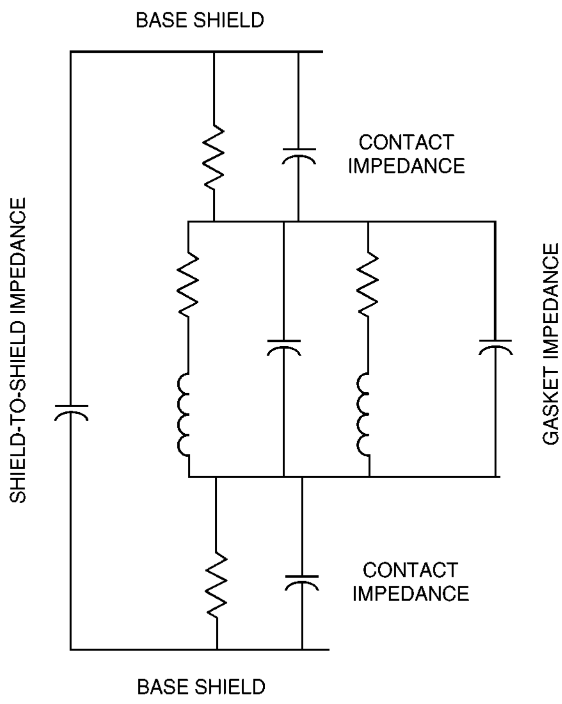


**Figure 2—Equivalent circuit of current path through a gasket**

Coupling through the gasketed joint will also be influenced by the length of the joint, the number and spacing of fasteners, and the degree to which the gasket material conforms to the joint’s gaps and irregularities

[8]The numbers in brackets preceded by the letter B correspond to those of the bibliography in Clause 10.

 

and maintains electrical continuity between the shield members. As the joint or seam approaches a resonant length, or as the spacing between fasteners approaches resonance, coupling through the aperture can be maximized or minimized according to the impedance match to the incident field.

Minimal power transfer from a source to a load occurs when their impedances are severely mismatched (i.e., high-to-low or low-to-high). Typically, the maximum mismatch is provided by an open or short circuit. Since the goal of a shield is to minimize the power transfer from a radiating source to either a susceptible load or the environment, the shield, including any gaskets, must present a high degree of mismatch to the impinging wave or to its load, which is likely to be free space. Both the impedance of the shield-gasket combination and that of the incident field affect this match.

## 5. Electromagnetic behavior of gasketed joints

A propagating electromagnetic wave has an impedance that is defined by Jordan [B8] as

$$Z_w = \frac{E}{H} \tag{1}$$

where

$E$ is the electric field component in volts per meter; and
$H$ is the magnetic field component in amperes per meter at the same point on the wave.

The intrinsic impedance, $\eta$, of any medium is defined as

$$\eta = \sqrt{\frac{j\omega\mu}{\sigma + j\omega\varepsilon}} \tag{2}$$

where

$\omega$ is the radian frequency of the field;
$\mu$ is the permeability of the medium;
$\sigma$ is the conductivity of the medium; and
$\varepsilon$ is the permittivity of the medium.

(In general, $\mu$ and $\varepsilon$ are complex quantities that contribute both phase shift and attenuation to waves passing through the medium. For the purpose of this discussion, however, no loss of generality arises by considering them to be real.)

In homogeneous, isotropic material, $\eta$ is a constant with the direction of propagation. In anisotropic material, $\eta$ is dependent upon the direction of wave travel and the polarization of the wave. Both types of material can exhibit an $\eta$ that varies with frequency.

In air, $\sigma = 0$, $\mu = \mu_0$, $\varepsilon = \varepsilon_0$, and

$$\eta_0 = \sqrt{\frac{\mu_0}{\varepsilon_0}} = 120\pi \approx 377\ \Omega \tag{3}$$

where

$\mu_0$ is the permeability of free space and is equal to $4\pi \times 10^{-7}$ H/m; and

$\varepsilon_0$ is the permittivity of free space and is equal to $8.85 \times 10^{-12}$ F/m.

In the far field of a source, $Z_w = \eta_0 = 377\ \Omega$. The far field is a distance that is dependent upon the source radiator geometry, and is typically defined as $\lambda/2\pi$ for thin, wire-type antennas and as $2D^2/\lambda$ for other types of radiators. In either case, $\lambda$ is the wavelength of the radiated field, and $D$ is the largest dimension of the radiator. At closer distances, the impedance of the field is a function of the impedance of the generating source and of the separation from the source. In the near field, the electromagnetic field will be predominantly a high-impedance ($E >> H$) electric field or a low-impedance ($E << H$) magnetic field. Except for static (i.e., dc) fields, every electromagnetic field contains both $E$ and $H$ components. At separation distances that are short relative to a wavelength, the E-field component predominates near voltage sources (high impedance) while the H-field component predominates near current sources (low impedance). Examples of voltage sources are predischarge electrostatic fields, short monopole antennas, and unterminated PC board traces whose sources have rise times that are greater than 20 ns. Examples of current sources are ac power lines, loop antennas, transformers, inductors, and power supply traces on PC boards. As the distance from the source increases, the field impedance approaches that of the intrinsic impedance of the propagating medium, as illustrated in Figure 3. Thus, in the far field, the impedance of the radiated wave approaches $\eta_0$. In the near field, $Z_w > \eta_0$ for electric field sources, and $Z_w < \eta_0$ for magnetic field sources.

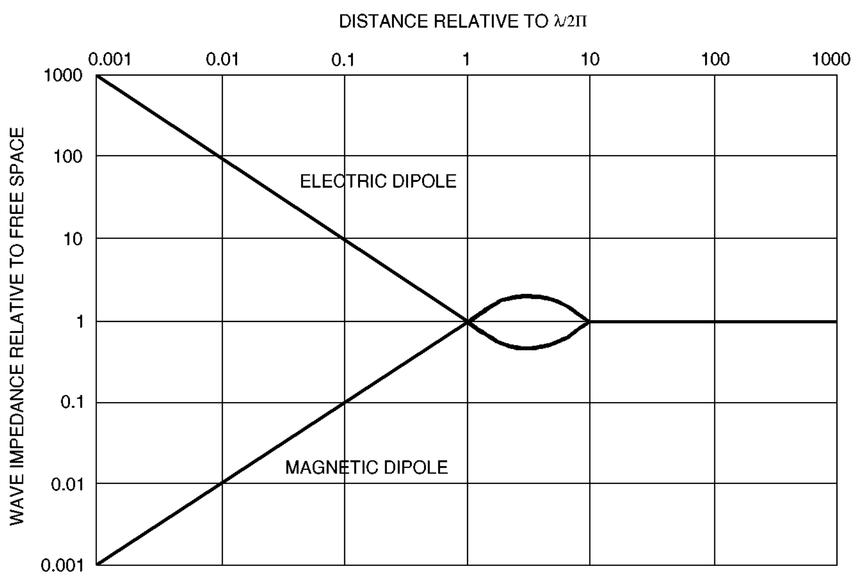


**Figure 3—Field impedance as a function of distance from the source**

Once installed in its final application, the typical gasket will be exposed to both electric and magnetic fields, as well as to plane waves. Both voltage and current sources exist inside equipment. At sufficiently high frequencies, plane waves may also impinge on the shield from inside the enclosure. The equipment may be located near both voltage and current sources. It may also be exposed to plane waves from the environment. Thus, in general, it is difficult to say what the impedance of the illuminating field will be.

In the typical shield, $\sigma >> \omega\varepsilon$. Thus, the shield impedance, $\eta_s$, becomes

$$\eta_s = \sqrt{\frac{j\omega\mu}{\sigma}} \tag{4}$$

which is significantly less than $\eta_0$ and, consequently, far less than the impedance of a field that is produced by a voltage source. Note, however, that unless $\mu > \mu_0$, as it is for ferrous materials and for special high-permeability materials, $\eta_s$ may not be low relative to the impedance of a field that is produced by a current source, particularly at audio frequencies.

When a "canonic" (plane, cylindrical, or spherical) electromagnetic wave impinges on a shield, part of the wave is reflected and part is transmitted into the shield, as described by Schelkunoff [B22]. The portion of the wave that is reflected is given by

$$\frac{E_r}{E_i} = -\frac{H_r}{H_i} = \frac{Z_{\text{shield}} - Z_w}{Z_{\text{shield}} + Z_w} \tag{5}$$

where

$E_i$ and $H_i$ are the components of the incident field;

$E_r$ and $H_r$ are the reflected components;

$Z_{\text{shield}}$ is the shield impedance; and

$Z_w$ is the impedance of the incident wave.

The portion of the wave that is transmitted into the shield is given by

$$\frac{E_t}{E_i} = \frac{2Z_{\text{shield}}}{Z_{\text{shield}} + Z_w} \text{ and } \frac{H_t}{H_i} = \frac{2Z_w}{Z_{\text{shield}} + Z_w} \tag{6}$$

For illustration purposes, consider a plane wave that impinges on a semi-infinite sheet of a good conductor ($\sigma >> \omega\varepsilon$). Here, $Z_w$ is $\eta_0$ and $Z_{\text{shield}}$ is $\eta_s$. Since the shield impedance is much lower than the wave impedance, the field-reflection coefficients of Equation (5) can be simplified as follows:

$$\frac{E_r}{E_i} = \frac{\eta_s - \eta_0}{\eta_s + \eta_0} = \frac{\frac{\eta_s}{\eta_0} - 1}{\frac{\eta_s}{\eta_0} + 1} \approx \frac{0 - 1}{0 + 1} = -1 \tag{7}$$

Thus, for a good conductor, the reflected E-field component is approximately equal in amplitude and opposite in phase to the incident E-field. The reflected H-field component is nearly equal in amplitude to, and in phase with, the incident H-field (i.e., $H_r / H_i \approx 1$). Similarly, expressing Equation (6) as

$$\frac{E_t}{E_i} = \frac{2\eta_s}{\eta_s + \eta_0} \approx 0 \text{ and } \frac{H_t}{H_i} = \frac{2\eta_0}{\eta_0 + \eta_s} \approx 2 \tag{8}$$

shows that $E_t$ inside the sheet will be very small; and $H_t$ at the surface (i.e., the surface current density, $J_s$) will be approximately twice $H_i$. Note that, although this relationship is derived using only plane waves for simplicity, the conclusion is valid for waves of all impedances.

Since the current induced in a conductor by a changing magnetic field is orthogonal to the field, that portion of $H_i$ that is parallel to a gasketed seam induces a current in the surface of the shield that is perpendicular to the seam. This current flows through the gasket and produces a voltage, $V_0$, across the output face, as illustrated by Figure 4. (The dashed line of Figure 4 depicts the decrease in amplitude experienced by a wave that is propagating through the lossy gasket, where the path through the gasket is significantly greater than the skin depth in the gasket material.) The voltage developed across the gasket, divided by the current per-unit length, is defined as the transfer impedance, $Z_t$, of the gasket, such that

$$Z_t = \frac{V_0}{J_s} \tag{9}$$

Note that the units of $Z_t$ are ohm meters, since the units of $J_s$ are amperes per meter.

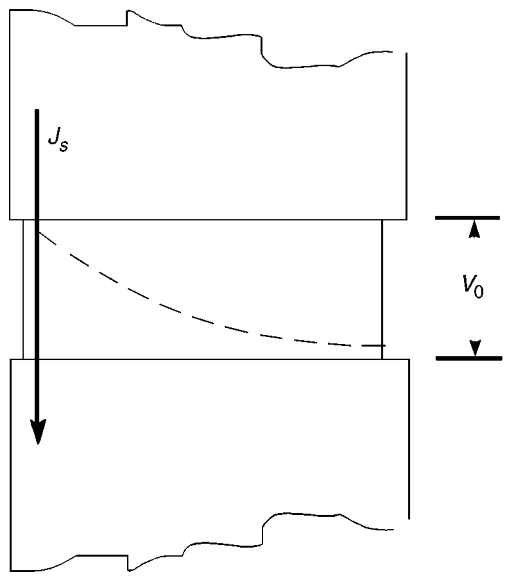


**Figure 4—Relationship between output voltage and input current in a uniform gasket**

The field attenuation, or shielding effectiveness (SE), of a gasketed seam is directly related to $Z_t$, see Kunkel [B9]. For example, consider a semi-infinite shield with a straight seam that is parallel to the H-field vector. The current that is induced in the shield will flow through the gasket, assuming that no paths around the seam exist. $H_i = E_i/Z_w$. Since $J_s = 2H_i$, the voltage, $V_0$, across the gasket will be

$$V_0 = J_s Z_t = \frac{2E_i}{Z_w} Z_t \tag{10}$$

As an example of the shielding effectiveness of a gasket of uniform height and thickness ($t$) in a simple configuration, note that $E_0 = V_0/t$, and invoke the standard definition for SE:

$$\mathrm{SE} = 20\log_{10}\frac{E_0}{E_i} = 20\log_{10}\frac{2Z_t}{Z_w t} \tag{11}$$

Thus, knowing the transfer impedance of the gasket and its thickness, the shielding effectiveness of a gasketed seam can be determined if the impedance of the impinging wave is known. However, as pointed out earlier, the fields that are incident on installed gaskets are typically unknown and can vary from a very low impedance to a very high impedance. Thus, using $Z_t$ to predict the shielding effectiveness of a gasketed seam to an incident field of unknown impedance can produce misleading results.

 

To evaluate a gasket's behavior under the wide range of wave impedances that it encounters in use, radiated testing techniques are employed. The radiated techniques typically employ one or more metal cavities wherein energy is coupled through a wall via a seam that contains the gasket under evaluation. The gasketed seam is exposed to low-impedance magnetic fields, high-impedance electric fields, and plane waves. The gasket commonly is placed underneath a cover plate that is positioned over an aperture in the wall. Straight slots are also used. Electric-field monopoles, magnetic loops, and plane-wave radiators are used to generate fields on one side of the aperture or slot. The fields coupled to the other side are measured with and without the gasket in place. Since the gasketed seam is strongly polarized, the coupled fields may be measured at a variety of viewing angles.

Figure 5 is a cross-section of a typical seam.

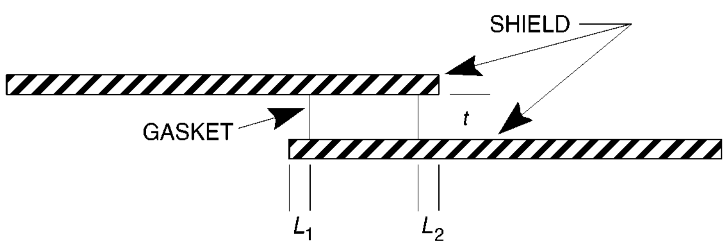


**Figure 5—Cross-section of a gasketed seam with uniform separation between base materials**

When

a) The gasket fills the overlap between the two surfaces (i.e., $l_1$ and $l_2 = 0$);
b) $Z_t$ is small compared to the radiation resistance [$R_e(Z_{rad})$] per unit length seen by an infinitely long seam that looks into free space; and
c) The gasket thickness, $t$, is uniform;

the power radiated per unit length by this seam is, from Quine and Pesta [B21],

$$P_{rad} = |V_0|^2 R_e\left(\frac{1}{Z_{rad}}\right) = |V_0|^2 G_{rad} = |J_s|^2 |Z_t|^2 G_{rad} \tag{12}$$

Here, $Z_{rad}$ is the radiation impedance and $G_{rad}$ is the real part of the admittance:

$$Y_{rad} = \frac{1}{Z_{rad}} = G_{rad} + jB_{rad} \tag{13}$$

For free space (see Marcuvitz [B12]),

$$G_{rad} = \frac{\pi}{\eta_0 \lambda} \tag{14}$$

An alternative expression for $P_{rad}$ is

$$P_{rad} = \eta_0 |H_i|^2 W_{eff} \tag{15}$$

where $W_{\mathrm{eff}}$ (called “ETW” in Quine and Pesta [B21]) is the effective transmission width of the gasketed seam.

Realizing that $J_s = 2H_i$, and combining Equations (12), (14), and (15), produces

$$|2H_i|^2|Z_t|^2\left(\frac{\pi}{\eta_0\lambda}\right) = \eta_0|H_t|^2W_{\mathrm{eff}} \tag{16}$$

from which

$$W_{\mathrm{eff}} = \frac{4\pi|Z_t|^2}{\eta_0^2\lambda} \tag{17}$$

If the power loss through the gasket aperture is small relative to the wall losses of the enclosure (see Quine [B17]), the SE of an enclosure that contains a gasket can be expressed in terms of $Z_t$ (from Quine [B16] and [B21]) as

$$\mathrm{SE} = \frac{3\pi V}{W_{\mathrm{eff}}l_g\lambda Q} = \frac{3\eta_0^2V}{4l_gQ|Z_t|^2} \tag{18}$$

where

- $V$ is the volume of the enclosure;
- $l_g$ is the length of the gasket; and
- $Q$ is the ratio of energy stored in all resonant modes in the enclosure to that which would be stored with no losses.

Equation (18) gives the shielding effectiveness of an enclosure that contains a gasket that is characterized by its effective transmission width. Note that the SE exhibited by the enclosure is directly proportional to the volume of the enclosure in which the gasket is installed, and is inversely proportional to the $Q$ of the enclosure, the length of the gasket, and the square of the magnitude of the transfer impedance of the gasket. Consequently, different values of SE will be observed with different sized enclosures. Variations in the measured SE can also result from additions of new test instrumentation into the test chamber or from relocations of existing instrumentation, both of which could change the $Q$ of the enclosure or could change the mode structure.

Equation (18) also indicates that the same gasket, under identical conditions of mounting, environmental exposure, aging, fastener torque, etc., will behave differently between a small and a large electronics cabinet, or between an enclosure that is filled with electronics (low $Q$) and an empty (high $Q$) enclosure, such as a measurement chamber.

## 6. Gasket measurement techniques

Standardized measurement techniques consist of the transfer impedance measurement of ARP 1705-1981 and the aperture transmission implementations of ARP 1173-1988, Def Stan 59-103 (17-Sep-93), and MIL-G-83528B (1993). Salient features of these techniques are listed in Table 1.

Each technique possesses particular strengths and offers unique advantages in specific situations. For example, the technique of ARP 1705-1981 provides a direct indication of the transfer impedance of the gasket or of a gasketed joint and, consequently, of the H-field attenuation through the joint. If the impedance of the

**Table 1—Comparison of standardized gasket measurement techniques**

| | Measurement technique | | | |
|---|---|---|---|---|
| | ARP 1705-1981 | ARP 1173-1988 | Def Stan 59-103 (17-Sep-93) | MIL-G-83528B (1993) |
| Measurement principle | Current injection | Aperture attenuation | Aperture attenuation | Aperture attenuation |
| Parameter measured | Transfer impedance | *E*/*H*/Plane-wave attenuation | *E*/*H*/Plane-wave attenuation | *E*/*H*/Plane-wave attenuation |
| Unit of measure | dB/Ω-m | dB | dB | dB |
| Test sample configuration | Circular | Rectangular | Circular | Rectangular |
| Sample size | 150 mm diameter | 300 × 300 mm | 409 mm diameter | 610 × 610 mm |
| Frequency range | dc to 2 GHz | 400 Hz to 10 GHz | 10 kHz to 18 GHz | 20 MHz to 10 GHz |
| Typical dynamic range | 60–150 dB | 60–100 dB | 60–120 dB | 60–120 dB |
| Typical repeatability | ± 2 dB | ± (6–20) dB | ± (6–20) dB | ± (6–33) dB |

incident field is known, transfer impedance can be used in Equation (11) to determine the shielding effectiveness of the gasketed seam.

The aperture transmission measurement techniques provide results in decibels, which are very attractive to equipment and system designers who tend to visualize gasket performance in such terms. However, the field attenuation that is exhibited by a gasketed seam is strongly dependent upon the nature of the electromagnetic field on the illuminated side of the seam, and on the particular field component that is being measured on the "receive" side of the seam. The effects of the aperture that is used for measurements can overshadow the attenuation that is provided by the gasket alone. Because of the many factors that can affect measurement results, data taken under different test conditions can be markedly different. Furthermore, test results are hard to relate to the gasket's intrinsic transfer impedance.

The standardized aperture transmission techniques measure the signal through the gasketed aperture at specific orientations and look angles. As noted above, however, the signal coupled through the gasket is strongly influenced by the measurement antenna locations relative to the aperture and by the surrounding enclosures. To fully characterize the coupling through the gasket, the illuminating antenna is often moved about, so as to expose the seam to various incident field conditions, and detailed field measurements over the hemispherical volume on the output side of the gasketed joint are made. Since each possible antenna pairing involves a measurement of the coupling with and without a gasket present, the level of effort required to perform the evaluation is high.

The effects of enclosure and fixture resonances must be recognized. Fixture resonances currently limit the transfer impedance technique to below about 2000 MHz. The chambers used with radiated techniques are resonant cavities. Once their longest dimension (typically the distance between diagonally opposite corners) reaches one-half wavelength, resonant modes exist from that frequency upward. Some of these resonances can be very sharp. Consequently, very small changes in antenna position inside the chamber can produce very large changes in the measured signal level. In addition, the size of the aperture influences the attenuation of the field that is coupled through it. If the aperture is significantly less than one wavelength, the attenuation through it is very high, and is inversely proportional to frequency. This attenuation limits the lowest frequencies that can be effectively measured, and can restrict the types of gaskets that can be accurately evaluated. Chamber resonances and aperture dynamic range requirements tend to restrict radiated tests to above about 200 MHz for the size of chambers and apertures that are typically used in the measurement of gaskets.

Between about 200 MHz and 2000 GHz, the potential for direct comparison between the standardized techniques exists. Both below and above these overlap regions, however, direct comparison is difficult. For example, below the overlap region, the transfer impedance technique provides information on the plane wave and magnetic field behavior of the gasket, whereas the radiated techniques largely provide information on electric and magnetic field behavior. Above the overlap region, the transfer impedance fixture exhibits strong resonances, which make comparison of its results with the plane-wave data of the radiated techniques difficult.

## 6.1 Transfer impedance

The gasket illustrated in Figure 5 is a two-port network with a 2 × 2 impedance matrix that has components of $Z_{11}$, $Z_{22}$, $Z_{12}$, and $Z_{21}$. $Z_{11}$ is the input impedance and $Z_{22}$ is the output impedance of the gasket. The mutual impedances, $Z_{12}$ and $Z_{21}$, are both equal to the transfer impedance, $Z_t$. With sufficient attenuation (at least 15 dB or so) through the gasket, $Z_{11}$ is approximately equal to the characteristic circuit impedance of the parallel-plate transmission line that is filled with the material comprising the gasket. Thus,

$$Z_{11} = \eta_g t / l_g$$

where

$\eta_g$ is the characteristic wave impedance, as determined by Equation (2), for the gasket material;
$t$ is the thickness of the gasket between the plates; and
$l_g$ is the gasket length.

Since transfer impedance is a mathematical concept only, $Z_t$ is not a physical resistor that can be measured directly. Its behavior, however, can be effectively characterized with the ARP 1705-1981 fixture of Figure 6. The coaxial transfer impedance test fixture characterizes the $Z_t$ of the gasket by forcing a current to pass through an outside boundary of the gasket and by measuring the voltage drop across the inside boundary.

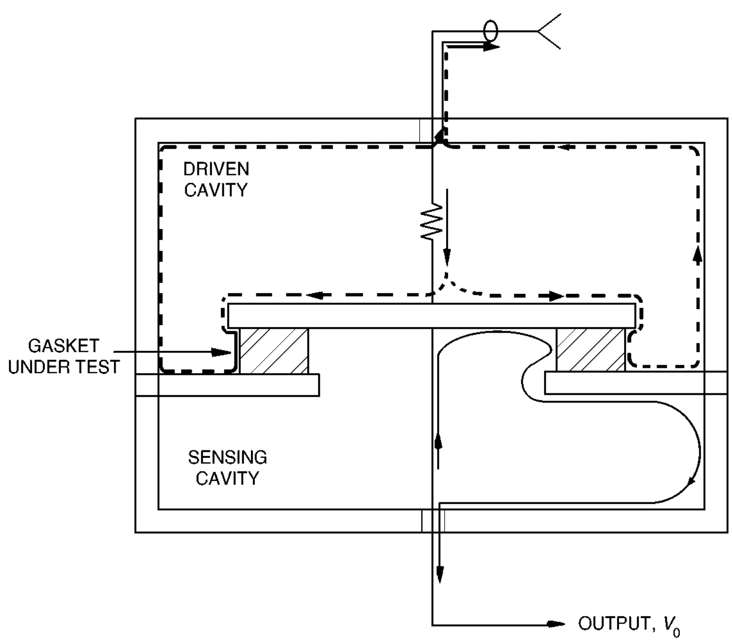


**Figure 6—ARP 1705-1981 coaxial transfer impedance test fixture**

If the dimensions of the gasket are small relative to wavelength, and the gasket is electromagnetically homogenous across the aperture, then the current induced in the shield may be assumed to flow uniformly through the gasket. Under these conditions, $Z_t$ may be viewed as a simple resistor. Figure 7 is the equivalent circuit of the transfer impedance test fixture of ARP 1705-1981. The gasket-under-test is represented by $Z_g$. The fixture is driven with a signal generator that has a source voltage of $V_s$ and an impedance of $Z_s$. The voltage of the applied signal and the voltage developed across the gasket are measured with a receiver that has a characteristic impedance of $Z_r$. A series resistor, $Z_f$, is incorporated into the fixture to provide a proper load to the source, to establish a common measurement reference, and to ensure that the current through the gasket is independently determined. $Z_f$ is chosen such that it is much larger than $Z_g$. The source voltage and current, $V_s$ and $I_s$, therefore remain constant with variations in $Z_g$. Thus, the voltage, $V_0$, developed across $Z_g$ is directly proportional to $Z_g$. The current, $I_g$, through the gasket must first be determined. Note from the circuit of Figure 7 that

$$I_g = \frac{V_s}{Z_s + Z_f + Z_g} \tag{19}$$

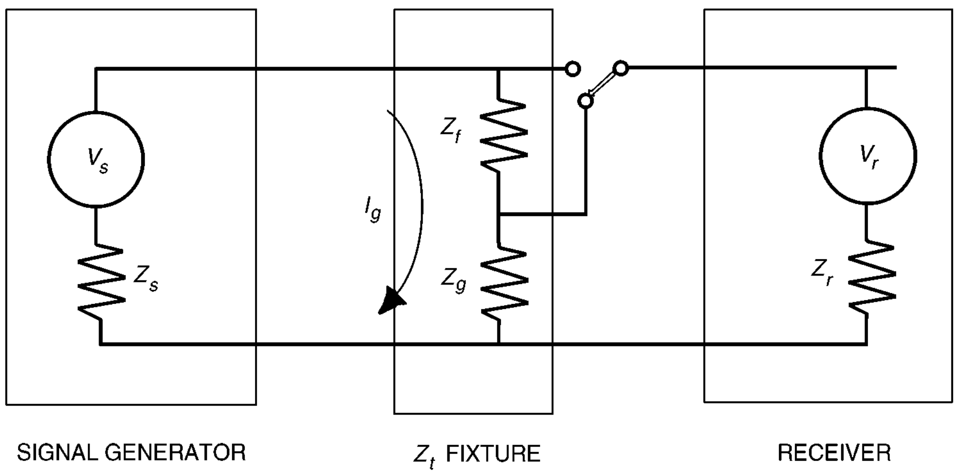


**Figure 7—Simplified representation of the transfer impedance measurement technique**

Typically, $Z_f$ is 50 Ω. Then, if $Z_g$ is much less than 50 Ω, $I_g$ can be measured directly by using a 50 Ω receiver that is connected across $Z_f$ and $Z_g$, as shown by the upper switch position in Figure 7. Under these circumstances, $I_g \approx V_r/50$, where $V_r$ is the voltage measured across $Z_f$ plus $Z_g$. Next, the receiver is switched to the lower position in Figure 7, so as to measure the voltage, $V_0$, developed across $Z_g$, as illustrated in Figure 6. $V_0$ is equal to $I_g \times Z_g$ or

$$V_0 \approx \frac{V_r Z_g}{50} \tag{20}$$

Thus,

$$Z_g \approx 50\frac{V_0}{V_r} \tag{21}$$

 

Since

$$Z_t = Z_g \times l_g = 50\frac{V_0}{V_r} \times l_g \tag{22}$$

the measured voltage ratio is multiplied by 50 and by the length of the gasket sample to produce the transfer impedance in ohm meters.

The transfer impedance test fixture of ARP 1705-1981 is typically constructed as two cylindrical cavities, with the gasket-under-test providing the coupling between them. The input cavity is driven with a 50 Ω coaxial signal source. A 50 Ω series resistor inside the fixture properly terminates the source and ensures that the current through the gasket is determined by the source. The voltage that is developed across the gasket is monitored with a coaxial attachment to the output cavity. Thus, $50V_0/V_r$ times the length of the gasket sample is a direct indication of the transfer impedance of the gasket.

$Z_t$ provides an excellent indication of the relative quality of the gasket, and is extremely useful for comparing different materials and construction techniques. Unless the test fixture surfaces, mounting techniques, and fasteners closely emulate those of the equipment in which the gasket is used, however, test results can be misleading.

To ensure that the transfer impedance measured is that of the gasket and not of the contact surfaces, the fixture's mating surfaces should be plated with a noncorrosive and highly conductive material, such as gold, to maximize the conductivity between the fixture and the gasket-under-test. If the transfer impedance of the as-installed gasket is desired, the fixture's gasket contact surfaces should be of the same material as the final enclosure, should have the same coatings, and should be machined in the same way. The effects of aging, corrosion, or other operating and storage conditions on the gasket's transfer impedance can be determined by subjecting the gasket and fixture contact plates to various environments.

## 6.2 Relative aperture transmission

Three radiated measurement techniques are in current use. All are based on the aperture transmission principles, and are derivatives of MIL-STD-285 (1956) [B13]. These techniques are ARP 1173-1988, MIL-G-83528B (1993), and Def Stan 59-103 (17-Sep-93).

MIL-STD-285 (1956) [B13] was first approved in 1956 as a US military standard for measuring the shielding effectiveness of military shelters. It was in use until it was cancelled in favor of IEEE Std 299-1991. ARP 1173-1988 was developed as an aerospace recommended practice (ARP) by the Society of Automotive Engineers (SAE) Committee AE-4 on Electromagnetic Compatibility. It was developed to measure the shielding effectiveness of EMI gaskets in general. MIL-G-83528B (1993) was developed as a procurement specification document for specific types of military conductive elastomer EMI gaskets. Shielding effectiveness test requirements are included along with many other electrical and mechanical requirements. Def Stan 59-103 (17-Sep-93) was developed as a means of standardizing gasket performance parameters and measurement methods. This standard addresses many types of EMI gaskets in use by the military and parallels MIL-G-83528B (1993) in many respects. Unlike MIL-G-83528B (1993), it imposes no performance requirements.

These techniques first establish a field reference level that radiates through an aperture in a high-performance shielded enclosure. Depending upon the implementation, the aperture may or may not have a metallic cover plate in place for the reference measurement. Next, the fields that are coupled through the aperture with the gasketed cover plate in place are measured. The difference, in decibels, between the two measured fields is defined as the shielding effectiveness of the gasket or gasket-plus-cover. Both measurements are made at discrete frequencies and for particular illuminating fields. The nature of the illuminating field varies with frequency and with the type of antenna that is used.

The EMI gasket measurement techniques contained in these standards consist of magnetic field, electric field, and plane-wave illumination of EMI gasketed joints. These gasketed joints consist of a metal cover that is attached to a metal flange, which forms the border of an aperture. The EMI gasket-under-test is installed in the cover-to-flange joint. The aperture is of fixed dimensions. Several types of antennas are used to cover the frequency range of the test, as well as the types of fields that must be generated and measured. Transmit and receive antennas are initially placed on opposite sides of the open aperture to create a reference electromagnetic field level. The EMI gasketed cover is then installed, and another field measurement is made of the gasketed joint with the antennas left in the same position. The difference between the two received field levels is defined as the shielding effectiveness of the EMI gasket, in decibels.

One of the measurement techniques (ARP 1173-1988) uses metal spacers between the cover plate and the flange to set up an additional reference measurement of the field level on either side of the slot that normally would be filled with the EMI gasket. The difference between this reference measurement and the gasketed cover measurement is referred to as the “shielding increase.” Similar modifications of the MIL-G-83528B (1993) measurement procedure, which are not yet part of the current issue of the document, are also in current use within the industry. These modifications involve the use of nonconductive spacers to create a similar aperture, and the use of nonconductive bolts to eliminate the effects of the fasteners on the measurement.

Figure 8 shows the setup for IEEE Std 299-1997 electromagnetic field reference measurements. In this case, the reference electromagnetic field level is taken with the transmit and receive antennas in free space, separated from each other by a fixed distance that is determined, in part, by the thickness of the cover plate. This type of field reference results in relatively high measured shielding effectiveness values for an EMI gasketed flange. The MIL-G-83528B (1993) procedure establishes a reference level, as shown in Figure 9, by aligning the transmit and receive antennas through an open aperture in the wall of a shielded room. This results in a lower reference level than for an IEEE Std 299-1997 measurement because of the aperture attenuation.

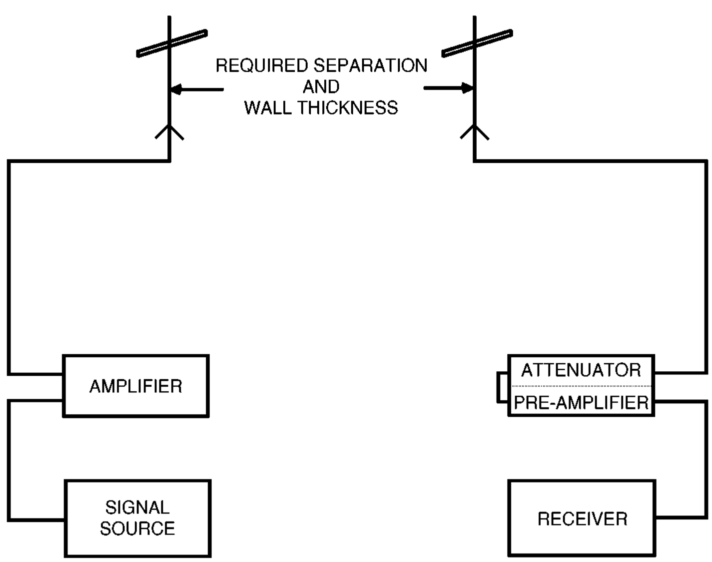


**Figure 8—IEEE Std 299-1997 shielding effectiveness reference level establishment**

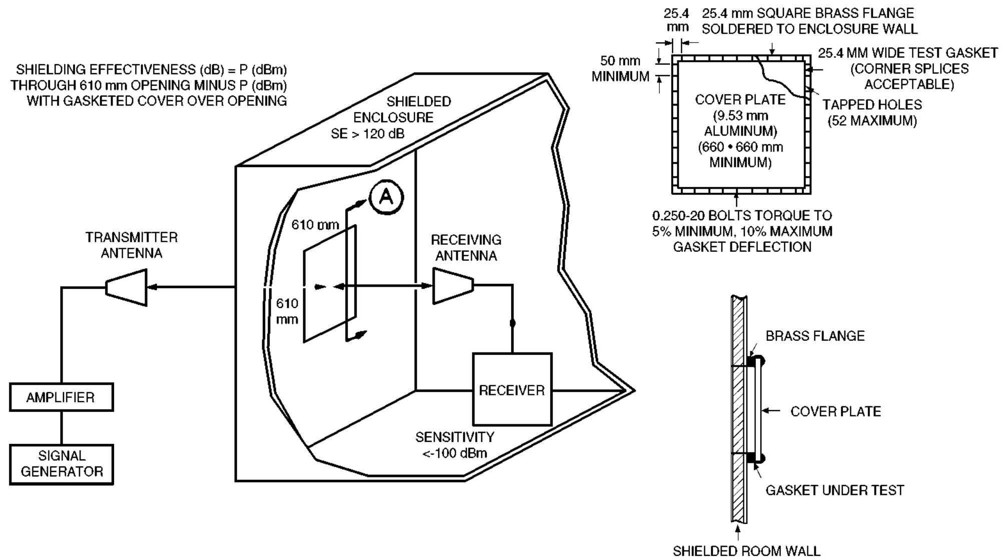


**Figure 9—MIL-G-83528B (1993) test setup**

ARP 1173-1988 uses two electromagnetic field reference levels. One is the same through-the-aperture measurement as for MIL-G-83528B (1993). The second involves measuring the electromagnetic field coupled through the slot or gap formed by the cover plate that is being held off its mounting flange by metallic spacers, but is fastened with nonconductive bolts. This significantly reduces the initial electromagnetic field reference level. Figure 10 shows the test setup.

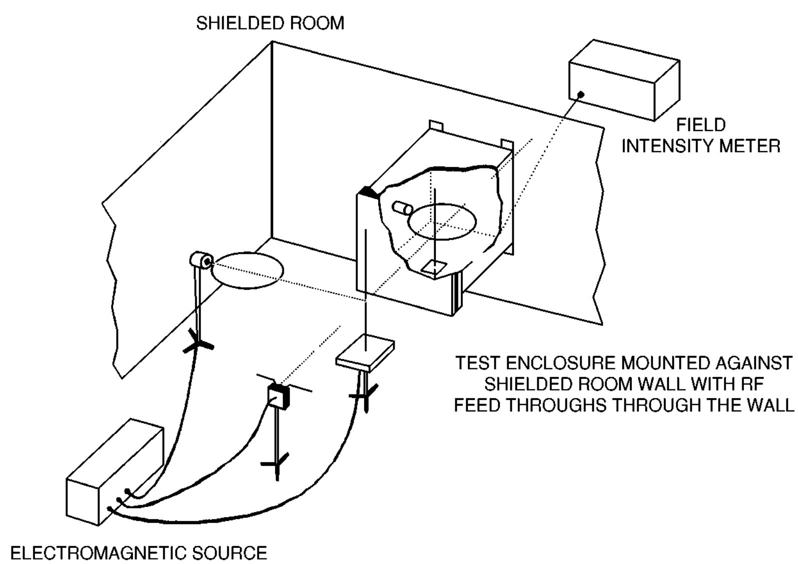


**Figure 10—ARP 1173-1988 test setup**

 

Def Stan 59-103 (17-Sep-93) also uses two electromagnetic reference levels. One is the same as the MIL-STD-285 (1956)/IEEE Std 299-1997 open field reference; the other is the same as the ARP 1173-1988 slot/gap reference measurement. Figure 11 shows the measurement aperture.

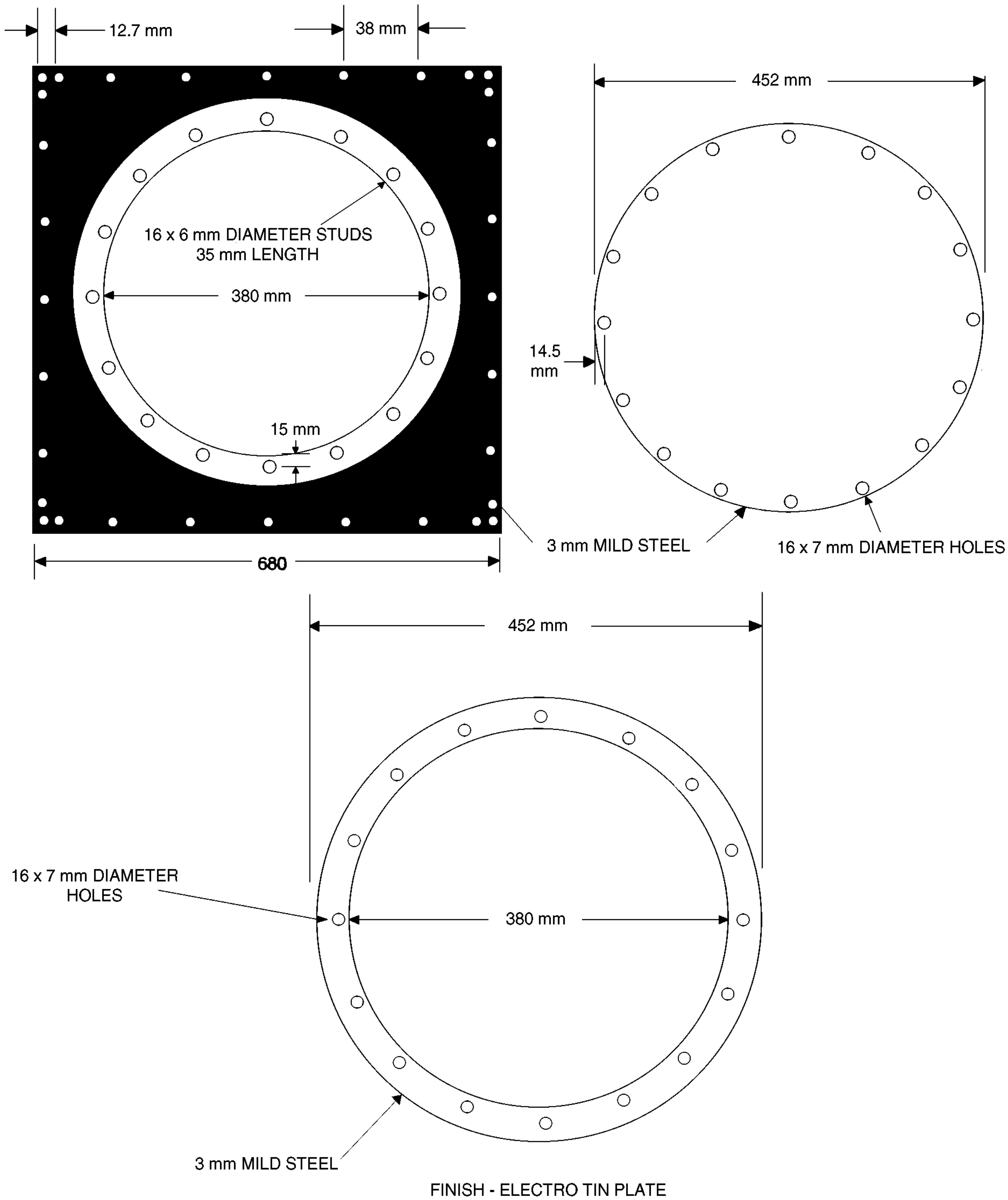


**Figure 11—Def Stan 59-103 (17-Sep-93) measurement aperture**

The antennas that are used for measurement consist of loops for magnetic field; dipoles, standard gain and ridged guide horns, biconicals, log spirals, and log periodic antennas for electric field; and standard gain or ridged guide horn antennas for plane-wave measurement. These different antennas are needed to generate the three different types of electromagnetic fields to be measured, as well as to cover the frequency range of measurement.

The aperture attenuation techniques define SE, in decibels, as

$$SE = 20\log_{10}\frac{E_1}{E_2} = 20\log_{10}\frac{H_1}{H_2} \tag{23}$$

where

$E_1$ or $H_1$ is the incident electromagnetic field on one side of the gasketed cover plate; and
$E_2$ or $H_2$ is the corresponding field component on the opposite side of the gasketed cover plate.

The E-field can be expressed in volts per meter or dBμV/m (decibels above a microvolt per meter). The H-field can be expressed in amps per meter or dBμA/m (decibels above a microampere per meter). The use of the logarithmic expressions for the electromagnetic field strengths allows for simple subtraction of the transmitted field strength value from the incident value.

ARP 1173-1988 also defines "shielding increase" as the difference between the amplitude of the electromagnetic field that radiates through the aperture that is formed by a cover plate and flange, and the amplitude of the electromagnetic field level that results from the fully gasketed cover plate.

Note that the different electromagnetic field reference levels among these three standards makes it difficult to correlate their results. The smaller the aperture that is used for the initial electromagnetic reference level, the smaller the dynamic range that is available for test. In the case of ARP 1173-1988, in which the reference level is taken through the slot or gap formed by the cover plate and flange, one is able to assess the metal cover plate's contribution to the shielding effectiveness measurement. This additional information allows an assessment of what the gasket contributes to the overall shielding effectiveness of the test joint. Since, however, ARP 1173-1988 uses metallic spacers under the cover plate, and because the cover plate is quite rigid, true EMI gasket performance is not fully evaluated.

The following tabulations show the relative differences in the tests among the three techniques:

a) ARP 1173-1988 test conditions:
   — *Test enclosure*—305 × 305 × 305 mm (12 × 12 × 12 in) (internal dimensions) 1010 steel, 6.35 mm (1/4 in) thick steel box, mounted to the internal wall of a shielded room.
   — *Cover plate*—381 × 381 × 9.5 mm (15 × 15 × 0.375 in) thick electroless nickel-plated flange with 0.025 mm (.001 in) maximum gap between the cover plate and the enclosure.
   — *Fasteners*—12 equally spaced, nonconductive fasteners with metallic spacers (washers) on each corner.
   — *EMI gasket-under-test*—square "picture frame" gasket with a developed length of 1.372 m (54 in).
   — *Test frequencies:*
      — *Magnetic field:* 400 Hz, 1 kHz, 14 kHz, 50 kHz, and 200 kHz.
      — *Electric field:* 1 MHz, 18 MHz, and 100 MHz.
      — *Plane-wave field:* 400 MHz, 1 GHz, 2 GHz, and 10 GHz.
   — *Receive antennas*—located inside test enclosure:
      — 203 mm (8 in) long antenna.
      — 203 mm (8 in) diameter loop antenna.
   — *Transmit antenna separation distance:*

    - *Magnetic loop and rod antenna:* 152 mm (6 in).
    - *Dipole and all other antennas:*1 m (39.4 in).
  - *EMI gasket measurement:*
    - Shielding increase due to EMI gasket (with and without the EMI gasket in the test joint).
    - Total shielding effectiveness.
  - *Calibration*—calibration gasket used to check uniformity of gasket pressure.

b) MIL-G-83528B (1993) test conditions:
  - *Test enclosure*—610 × 610 mm (24 × 24 in) aperture with 25.4 mm (1 in) brass flange soldered to the wall of a shielded room.
  - *Cover plate*—660 × 660 × 9.5 mm (26 × 26 × 0.375 in) 6061-T6 aluminum.
  - *Fasteners*—52 1/4–20 metallic bolts spaced at 25.4 mm (1 in) intervals, torqued to provide gasket deflection of 5% minimum and 10% maximum.
  - *EMI gasket-under-test*—25.4 mm wide × 1.75 mm thick × 660 mm × 660 mm (1 in wide × .062 in thick × 26 in × 26 in) "picture frame" gasket.
  - *Test frequencies*—20 MHz to 10 GHz (electric field); swept frequencies are encouraged, but the 1, 2, 4, 6, and 8 times multiple of each frequency decade is allowed.
  - *Receive antennas*—located inside shielded room (outside room optional): biconical, dipole, horn, and ridged guide horn antennas.
  - *Transmit antennas*—biconical, dipole, horn, and ridged guide horn antennas.
  - *Transmit antenna separation distance*—2 m (78.8 in) plus the thickness of the cover plate.
  - *Measurement*—total shielding effectiveness.

c) Def Stan 59-103 (17-Sep-93) test conditions:
  - *Test enclosure*—380 mm (15 in) circular aperture in 3 mm (0.12 in) thick mild steel, electro tin plated 610 × 610 mm (24 × 24 in) penetration plate mounted on the wall of a shielded room.
  - *Cover plate*—3 mm (0.12 in) thick mild steel, electro tin plated, 452 mm (18 in) diameter.
  - *Fasteners*—16 equally spaced, 6 mm (0.24 in) diameter metallic studs mounted on penetration a penetration plate.
  - *EMI gasket-under-test*— circular, "picture frame" shape, with 1.35 m (53 in) developed length, 36 mm (1.4 in) wide.
  - *Test frequencies:*
    - *Magnetic fields:* 10 kHz, 100 kHz, 1 MHz, and 10 MHz.
    - *Electric fields:* 100 kHz, 1 MHz, 10 MHz, 100 MHz, and 400 MHz.
    - *Plane-wave fields:* 1 GHz, 10 GHz, and 18 GHz.
  - *Receive antennas*—located inside the shielded room: 305 mm (12 in) magnetic loop.
    - Rod antennas for electric fields.
    - Dipole, Yagi, and horn antennas for plane-wave measurements
  - *Transmit antennas*—305 mm (12 in) loop, rod, dipole, Yagi, and horn antennas.
  - *Transmit antenna separation distance*—305 mm (12 in) from cover plate for loop and rod antennas for electric field and magnetic field tests, 1.83 m (72 in) from cover plate for other antennas for plane-wave tests.
  - *EMI gasket measurements:*
    - Shielding increase due to EMI gasket (joint tested with and without EMI gasket).
    - Total shielding effectiveness.

## 6.3 Alternative techniques

In addition to the standardized techniques for evaluating the performance properties of conductive gaskets, other approaches have been used or are under development. These variants encompass statistical characterizations of the fields coupling through gasketed joints, measurement of the total power radiated through the gasket aperture, adaptations of techniques used to measure the shielding effectiveness of planar materials, and modifications of existing techniques to accommodate different gasket configurations.

### 6.3.1 Reverberation chambers

The electromagnetic environments (EME) that occur in such places as aircraft avionics bays, rooms in which electronics are used, onboard ships, and in the streets of metropolitan areas are usually very complex, encompassing a wide range of amplitudes, angles of incidence, and phase relationships. Predictions (see Lehman [B10] and [B11]) and research results (see Freyer, et al. [B5]) have shown that the statistics of the EMEs of all complex cavities are the same. By deliberately "stirring" the fields on both sides of an aperture that contains the gasket, the power coupling through the gasket can be measured on a time-average basis. Since the statistics of the EME in a reverberation, or stirred-mode, chamber are expected to be the same as those experienced in operation, the results that are obtained will be the bounding case for the gasket in its in-service configuration, and the results should be repeatable when tested in different reverberation chambers.

The aperture transmission techniques expose the gasket-under-test to discrete transmit-antenna-to-gasket orientations (aspect angles) and polarizations. Reverberation or mode-stirred chambers (MSC), however, expose the gasket-under-test to randomized fields by varying the electromagnetic boundary conditions in the chamber (see Hatfield [B7]). The gasket-under-test is thus exposed to fields of all aspect angles and polarizations without having to rotate the gasket-under-test or change the transmit antenna position or polarization. Through automated measurements, a statistical description of the field coupling through the gasketed joint is obtained. The best case, worst case, and average, or mean, coupling are measured.

The basic concept of the reverberation chamber, or MSC, test method for gaskets (see Quine and Pesta [B21]) is illustrated in Figure 12. Two metal enclosures are coupled via an aperture in a common wall. The gasket to be tested is mounted under a cover plate over the aperture inside one of the enclosures. Each chamber is equipped with a paddle-wheel tuner and antennas. The rotation rates of the paddle-wheels are adjusted so that the speed of one paddle-wheel is high compared to that of the other. This allows for the measurement of the maximum coupled fields inside one chamber as a function of the other chamber's tuner position. Shielding effectiveness is defined as the ratio of the power that is transferred into the second chamber, with only a cover plate over the aperture ($P_{\text{baseline}}$), to the power that is coupled through the aperture with the gasket-under-test inserted between the cover plate and the chamber wall ($P_{\text{coupled}}$), such that

$$\text{SE (dB)} = P_{\text{baseline}}\ \text{(dBm)} - P_{\text{coupled}}\ \text{(dBm)} \tag{24}$$

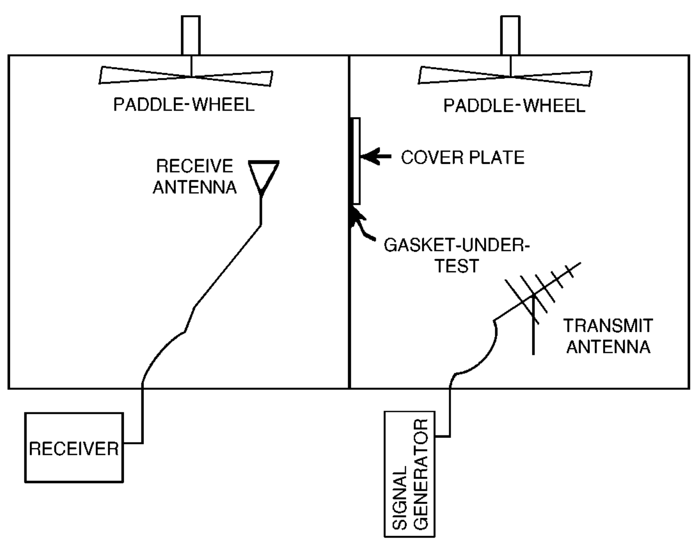


**Figure 12—Gasket measurements using reverberation chambers**

Both chambers must be operated above resonance so that a sufficient number of higher-order modes exist in each chamber for the proper “stirring” of the fields. Specifically, tests are conducted at frequencies at which 60 or more higher-order modes are excited (see Crawford and Koepke [B3]). For a rectangular fixture, the frequency at which 60 modes exist can be found by

$$N = 60 = \frac{8\pi lwh}{3\lambda^3} - \frac{(l + w + h)}{\lambda} + \frac{1}{2} \tag{25}$$

where

| | |
|---|---|
| *l*, *w*, and *h* | are chamber dimensions; and |
| $\lambda$ | is the wavelength. |

To illustrate the minimum dimensions required, a cubic ($l = w = h$) enclosure is assumed. Since the influence of the cubic term greatly outweights the other two, Equation (25) may be approximated as

$$\frac{8\pi}{3}\left(\frac{l}{\lambda}\right)^3 = 60 \tag{26}$$

This yields $l/\lambda = 1.9275$, or indicates that the minimum dimension of the chamber needs to be roughly two wavelengths to support the necessary number of modes for good characterization. The lowest frequency will be determined by the smallest chamber.

As the tuners in the chamber are rotated, the mode patterns are significantly changed. Both paddle-wheel tuners are typically rotated 360° in small steps using shielded motors. This results in a sufficient number of boundary condition changes to generate a field that is statistically uniform over one paddle-wheel rotation. Thus, during one paddle-wheel rotation, the gasket-under-test is exposed, on the average, to a uniform field level. RF energy that leaks into the second enclosure is similarly stirred with the second paddle-wheel tuner.

Improper placement and orientation of the transmitting and receiving antennas can adversely influence measurements. If a direct path exists between the transmit and receive antennas, or between the transmit antenna and the fixture, the fields that exist within the “test zone” will be biased and will not be statistically uniform over a single rotation of the paddle-wheel. In order to avoid biasing the measurements, the transmit antenna should be pointed toward a paddle-wheel tuner, or at a corner of the chamber, while avoiding a direct path through the test zone.

The “nested” implementation of the reverberation chamber technique is illustrated in Figure 13. In this approach, a small chamber is positioned inside a larger one. A typical test fixture for the nested reverberation chamber test is shown in Figure 14. In many cases, a single fixture can be adapted to test many gaskets. An example of adapting a fixture to test a shorter gasket is also shown in Figure 14.

The mode-stirred chamber test conditions are

a) RF-tight enclosures (conductive material bolted or welded together).
b) Equipment that is capable of generation RF signals over frequency ranges of interest, typically 200 MHz to 18 GHz.
c) Directional, linearly polarized transmit antenna (i.e., log periodic or waveguide horns).
d) At least one paddle-wheel tuner, with conductive vanes whose dimensions are large with respect to wavelength, that is mechanically coupled to a shielded motor or other device to turn the paddle-wheel.
e) For testing long gaskets, a solid conductive lid may be placed over the top of the gasket and fastened to the fixture with bolts. Nonconductive spacers are used when necessary to prevent damage to the gasket-under-test.
f) Measurements:
   - Power received by antenna(s) in the second chamber (baseline).
   - Power received by antenna(s) that are positioned in the fixture with the gasket in place.

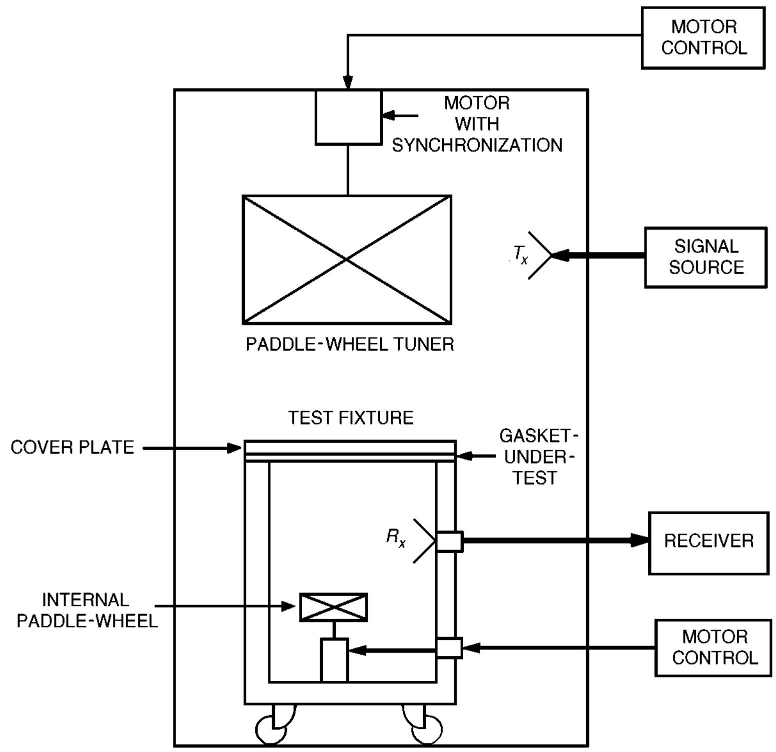


**Figure 13—Nested stirred-mode method for characterizing EMI gaskets**

Reverberation chamber tests can be very time-effective and cost-effective because testing to the same thoroughness using aperture transmission techniques requires the repeating of the test at a very large number of aspect angles and polarizations. In addition, if the EME to which the gasket-under-test is exposed in its in-service configuration is complex, reverberation chamber testing can be the most representative method by which to test the gasket.

The primary disadvantage of reverberation chambers is the reduced coverage at low frequencies. By using two large chambers, lower test frequencies can be used. From Equation (26), 3 m rooms permit testing down to 200 MHz. The lowest usable frequency for testing gaskets using the “nested” approach will be approximately 500 MHz because of the size of the smaller chamber.

### 6.3.2 Effective transmission aperture

This approach (see Quine [B17]) characterizes the gasket via a determination of the total effective power that is radiated through a gasketed aperture. From this power measurement, the effective transmission width ($W_{eff}$) can be determined. $W_{eff}$ is readily relatable to $Z_t$ [see Equation (17)]. The effective transmission aperture characterizes the power-coupling properties of an aperture in a manner that is analogous to characterizing a reflecting object via its radar cross-section. Each characterization is a measure of the relative amount of power that is transmitted or reflected by the aperture or object.

A conventional two-room, common-wall coupled reverberation chamber has been used to characterize gasketed seams in terms of their effective transmission area per unit length (see Quine, et al. [B18]). In this approach, the gasketed seam is mounted on the common wall between two chambers. Mode stirring is employed in one of the rooms. Rotatable linear-polarized excitation is employed, with absorbers in the

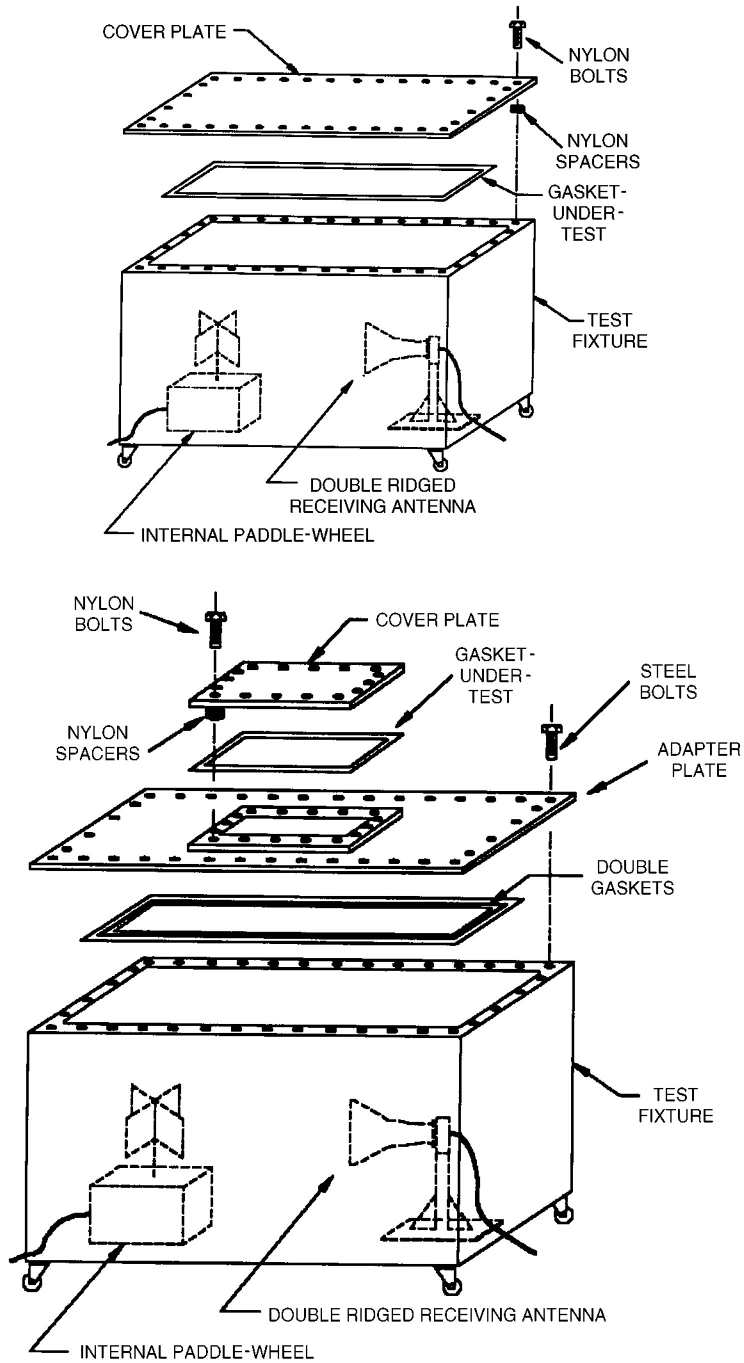


**Figure 14—Options for mounting the gasket-under-test**

smaller chamber to suppress resonances. Since the typical seam is highly polarized, a wave polarized with an H-field that is parallel to the length of the seam is used to characterize the behavior of the gasketed seam. To extend the technique to even lower frequencies, miniature H-field probes have been employed (see Quine, et al. [B19]) for determining the H-field vectors immediately on both sides of the gasket. Combined use of the probes and mode stirring allows for a determination of the effective transmission aperture per unit length of the gasket over a wide frequency range.

### 6.3.3 Modified ASTM D4935-89 (1994) fixture

ASTM D4935-89 (1994) utilizes an enlarged, tapered, coaxial transmission fixture for determining the plane-wave shielding effectiveness of thin, conductive planar materials. A proposed modification to this technique (see Adams [B1]) incorporates a gasket holder that is inserted into the ASTM D4935-89 (1994) fixture in place of the material holder. Shielding effectiveness is defined as the $10\log_{10}$ of the ratio of the power that is coupled through the fixture with the gasket present to the power that is coupled through the fixture without the gasket. The technique is simple to use. Swept-frequency instrumentation can be used to cover a broad frequency range in a single measurement. The results that are obtained appear to correlate well with those that are obtained with a transfer-impedance fixture. The primary disadvantages are that only plane-wave data are produced, and fixture resonances limit the use of the technique to below 2 GHz.

### 6.3.4 Slot aperture

This approach (see Peregrim [B15]) is a modification of MIL-G-83528B (1993) that substitutes a $3 \times 500$ mm ($0.12 \times 20$ in) slot for the $610 \times 610$ mm ($24 \times 24$ in) square covered aperture. In this way, the contribution of the cover plate to the total measured attenuation is removed, and only the contribution of the gasket is measured.

### 6.3.5 TEM-*t* and *H-t* fixtures

This technique (see Catrysee [B2]) is analogous to ASTM D4935-89 (1994) in that it inserts the sample to be measured in series with a transverse electromagnetic (TEM) mode transmission line device. With this technique, a square coaxial fixture is “cut” in the center, and the sample to be tested is inserted between the two halves. Coupling in and out of the test sample is via capacitance. Thus, E-field characteristics are measured. The output and input impedance of the fixture is 50 Ω. By varying the orientation of the test sample, polarization dependence can be evaluated. The frequency range of operation is reported to be 1–1000 MHz. To evaluate the magnetic coupling properties of the test sample, the *H-t* fixture modifies the center conductors of the TEM cell to incorporate small coplanar loops that are close to the test sample. The frequency range of the *H-t* fixture is said to be 1–1000 MHz. In both variations, swept frequency measurements can be accommodated.

## 7. Selecting a gasket measurement technique

Most of the present standards (ARP 1705-1981, ARP 1173-1988, etc.) define test details, such as fixture design, specimen configuration, mechanical loading conditions, and interface flange materials and surface treatments. It is unlikely that these test conditions and details will replicate the actual gasket application of interest. Therefore, each of the techniques should be considered as a “platform” from which minor modifications and adjustments can be made to more closely approximate the application in question. For example, the fixture might be modified to allow different cross-sections or compressive loading conditions to be tested. However, basic parameters of these techniques, such as aperture sizes, cavity dimensions, antenna setups, and frequency ranges should not be modified without a careful evaluation of the effects of such modifications on dynamic range, accuracy, repeatability, power requirements, and other factors.

### 7.1 Measurement reference

The decibel is used to cope with wide ranges of measured shielding effectiveness. In order to compare different gaskets in terms of decibel shielding effectiveness, they must be compared against a common reference. Unfortunately, the different techniques do not establish a common reference. For example, MIL-G-83528B (1993) establishes the reference field by performing a measurement of the field that transmits through a $610 \times 610$ mm open aperture, whereas ARP 1173-1988 defines the reference field as that coupled through a $305 \times 305$ mm aperture with the cover plate in place. In addition, MIL-G-83528B (1993) uses conductive fasteners, while ARP 1173-1988 uses nonconductive fasteners. As noted above, differences in aperture size, the presence of the cover plate, and the types of fasteners that are used can dramatically influence the coupling through the aperture. With the references being different, the separation of the effects of the aperture from those of the gasket can be very difficult.

A comparison of the results provided by four different measurement techniques on the same gasket samples (see Freyer, et al. [B6]) demonstrates that absolute decibel values of shielding effectiveness do not track across techniques for the same gasket, and that relative performance between gaskets does not correlate from technique to technique.

The units of $Z_t$ are ohm meters. Thus, to compare two gaskets in terms of their transfer impedances, their respective lengths must be known so that they can be normalized to the same length.

## 7.2 Sample configuration

Most of the existing test methods define a gasket specimen configuration in terms of size, shape, and cross-section. Table 1 describes the plan-view configuration and overall size of each method's gasket specimen. The terms "circular" and "rectangular" refer to plan view, not to cross-section. Since most specimens are cut from sheet material, they have rectangular cross-sections.

It is considered acceptable to vary the gasket cross-section, but not the overall (plan view) shape or size, for all standardized test methods. For example, gaskets with square, "O," "P," or hollow cross-sections could be substituted for the specified rectangular cross-section specimens. Such modifications may enhance the relevance of any of the methods for evaluating a particular gasket application.

## 7.3 Frequency range

The choice of frequency range is influenced by the end application. The type of field (E-field, H-field, or plane-wave) that impinges on a gasket during a radiated gasket test is wholly determined by

a) The type of source excitation (current or voltage)
b) The distance from the source antenna to the gasket-under-test
c) The source frequency

Detailed guidelines on antenna types, antenna-to-source distances, etc., for performing these tests may be found within the individual test standards.

Other factors that dictate the useful frequency range of radiated measurement approaches are related to both the size of the sample and the measurement environment. The size of the sample will directly determine the lower frequency limit of the measurements being made. The measurement aperture acts like a waveguide below cut-off or a high-pass filter. This means that frequencies below the cut-off frequency will be strongly attenuated. The dynamic range, consequently, will be severely limited in this region. In the case of MIL-G83528B (1993), this range is around 200 MHz for the 610 mm square aperture.

The measurement environment also affects the integrity of the measurements being performed. Most radiated gasket tests are made in simple shielded enclosures, since anechoic chambers are relatively expensive. At lower frequencies, in which the physical dimensions of the room are on the order of one-half wavelength, standing waves or resonances are produced. At the other end of the spectrum, numerous coupling modes may interact to compromise the base measurements. The use of reverberation chambers is recommended when maximum precision is required. This practice, however, once again carries a cost penalty.

Frequency limitations of a different variety are inherent in current transfer impedance approaches (such as ARP 1705-1981). Since the test fixture is coaxial, the energy propagates in a TEM mode that, in effect, can yield data down to dc, which is very useful. High-order modes in the fixture, however, presently limit the technique to below 2 GHz (see Freyer and Hatfield [B4]).

## 7.4 Dynamic range

Dynamic range refers to the difference, in decibels, between the minimum detectable signal with the gasket in place in the measurement fixture and the maximum signal that is coupled through the fixture without the gasket in place. The dynamic range will be bounded by the sensitivity of the measurement receiver and the power output capabilities of the signal sources, or by safety considerations or regulatory constraints. Dynamic range is predominantly a function of frequency. The direct impact of the cutoff properties of the aperture on dynamic range at frequencies of less than 200 MHz [see MIL-G-83528B (1993)] was mentioned previously.

Simplistically, the major contributors to dynamic range are source power, antenna gain, and receiver sensitivity, all of which vary with frequency. Suggested power levels typically are outlined for both signal generator and amplifier combinations in the standards themselves. Furthermore, typical antenna types are outlined. The choice of antennas is important because, for a given band, different gain antennas are available. Antenna gain is related directly to the illumination characteristics of the antenna.

Perhaps one of the most overlooked contributors to the dynamic range of a measurement is the integrity of the shielded room itself. Meaningful measurements require that the shielding effectiveness of the room be much greater than that of the gasket-under-test. Otherwise, extraneous signals or noise will mask the desired measurement.

These considerations suggest that it is desirable to estimate in advance what the anticipated shielding effectiveness of the gasket-under-test and its fixture is likely to be. Knowing this will help define the required parameters of the measurement approach.

## 7.5 Other considerations

It is often necessary and desirable to evaluate the effects of environmental exposures, mating flange finishes, or varying degrees of compression or gasket performance.

Because the transfer impedance technique employs a bench-top fixture with a small and easily removable gasketed test joint, it is especially suited to making measurements before and after environmental exposures. Although such evaluations can also be accomplished with the radiated techniques, some form of removable adapter plate is required; and the environmental chambers would need to be large enough to accommodate 300 mm or 610 mm square test flanges.

The evaluation of gasket performance as a function of mating flange surface (such as plating, coating, or finish roughness) can be accommodated by any of the standardized methods. Likewise, the mechanical modifications that used to evaluate various compression or deflection levels can be accomplished with any of the techniques. Fastener spacing, fastener torque, gasket cross-section, and mating flange flatness are some of the parameters that are typically modified for such evaluations. For gasket cross-sections that can be deflected with low compressive force, metal fasteners can be replaced with plastic fasteners to eliminate the contribution of the fasteners to the field attenuation.

The type and location of fasteners is important. Metal fasteners establish alternative paths for current to flow around the gasket. However, some users may want conductive fasteners to reflect actual usage in equipment. Conductive fasteners will cause fixture resonances at those frequencies at which the spacings are odd multiples of half wavelengths. Consequently, fixtures that have different fastener spacings may produce markedly different results.

With all other factors remaining constant, the power that is transmitted through a homogeneous gasket is proportional to its length. Thus, a fixture that employs long gaskets will show less shielding effectiveness than a fixture that employs short gaskets. So long as the gasket behaves as a uniformly distributed impedance across the measurement aperture, its transfer impedance, its effective transmission area, or its shielding effectiveness can be normalized to unit length. If, however, the measurement apparatus or the gasket itself exhibits resonances, unit length data can be unreliable.

## 8. Repeatability

All gasket measurements exhibit variations from test to test and from sample to sample. These variations are caused by differences in test setups, normal variations in test instrumentation, differences between test samples, and aging and environmentally induced changes in the samples. The variations between the results that are provided by different test techniques and by different test setups can easily be greater than those that arise from the gasket itself. Differentiating between these variations can be difficult.

Test-to-test variations arise from normal differences between instruments, from differences between transmitting and receiving antennas (including their positions) and, primarily, from differences between test techniques. Instrumentation-related variations include those variations that are caused by line losses, impedance matches between instruments, cables and antennas, and cable positioning. These line losses and impedance mismatches typically produce 2–6 dB variations between different test setups, but less than 1 dB variation between test samples that are measured with the same test setup. Cable positioning, however, can be critical during radiated measurements, and can easily cause 10–20 dB variations in test results. To minimize variations due to cable position, all signal and power cables must remain fixed in place throughout a measurement run.

The differences that are caused by the use of different test techniques can be dramatic. With the aperture transmission techniques, for example, the shielding effectiveness of a gasket that is measured with a pair of monopole (electric field) antennas will likely be much higher than that measured with a pair of loop (magnetic field) antennas. The results produced by these tests may not appear consistent with the results that are obtained with plane-wave exposure. Plane-wave tests that are performed with the aperture attenuation techniques use a variety of antenna types, such as horn, biconical, spiral, and log periodic antennas. The uniformity of the exposure of the gasket by the various antenna types varies with frequency and distance from the test sample. At those frequencies at which the gasketed aperture or the gasket itself behaves as a multimode antenna, in particular, only slight differences in separation distance or incidence angle can produce large changes in the received signal level (i.e., in the apparent shielding effectiveness of the gasket).

Unless test chambers are anechoic, they will exhibit very high $Q$s at resonances. Resonant effects, which can be significant from approximately 0.8 $f_r$, or about 85 MHz for a $2 \times 2 \times 2$ m enclosure, can result in changes of 20–40 dB in the received signal level that arises from very small changes in the location of the antenna in the chamber. In other words, small changes in the position of an antenna between samples, between test runs, or between test sites can produce large changes in the apparent shielding effectiveness of a test sample. In a similar vein, at frequencies at which the transfer impedance fixtures are resonant, small variations in fixture size or geometry can result in significant differences being produced by different test fixtures.

Correlations between shielded room sites can be difficult due to differences in the sizes of the shielded room and/or test setups. The presence of test personnel inside the enclosure, and their relative positions, can affect measured signal levels. Repeatability between measurements using the same shielded room site can be kept within 6 dB with attention to the details of the measurement procedures. Even this is difficult if different personnel perform the test.

Surface geometry and surface conditions of both the gasket and the fixture can be responsible for wide differences in test results. If the test fixture is bare aluminum, for example, it will have a very thin, nonconductive oxide film over the contact surface. Metallic gaskets that “bite” through this film will show much higher values of shielding effectiveness at lower frequencies than those that cannot penetrate the oxide film on the fixture. Some conductively loaded polymers (such as those loaded with nickel-coated graphite particles) have a particular morphology that allows excellent bite-through of oxide-coated surfaces. Environmental exposure can cause significant changes in the surface conditions of the gaskets themselves.

The reverberation chamber approach accepts that variations occur along the length of the gasket, and seeks to measure the maximum coupling through the gasket by collecting a statistically significant number of samples. Repeatability of reverberation chambers is typically on the order of 3–6 dB.

## 9. Measurement uncertainty

Measurement uncertainty is a range above and below a measured value that contains, with a specified probability, the true value of a measurand. The user of measured data must understand that the results obtained by different investigators will vary because of differences in the instrumentation, the measurement technique, and even in the requirements of the standard used to perform the test itself.

Most uncertainties are estimated based on the probability distributions that are assumed for, or assigned to, the contributing quantities, the use of the tolerances of the instrumentation, the measurement setup variability, and the technique of the tester in performing the test.

Typically, the overall uncertainty is estimated in part by identifying uncertainties and tolerances in the instrumentation chain that is used in performing each of the techniques shown in Table 1 of this guide. The figures associated with each technique show the basic components of the instrumentation chain. Each component will need to be evaluated as to its individual uncertainties. The most common guidance document for such evaluations is NIS 81 [B14].

Another component of uncertainty is based on the variability of repeated measurements. In Table 1, this has been estimated for each of the techniques shown. By combining this result with the estimation of the instrumentation uncertainty, using the technique contained in NIS 81 [B14], the overall measurement uncertainty can be estimated. The measurement uncertainty associated with a set of data should be provided in accordance with NCSL RP-12 (4/95). If not, the user should request it.

## 10. Bibliography

[B1] Adams, J. W., “Electromagnetic Shielding of RF Gaskets Measured by Two Methods,” *Proceedings of the 1992 IEEE International Symposium on Electromagnetic Compatibility*, Aug. 1992, pp. 154–157.

[B2] Catrysee, J., “New Test Cell for the Characterisation of Shielding Material in the Far Field,” *IEE Conference Publication No. 326*, 1990, pp. 62–67.

[B3] Crawford, M. L., and Koepke, G. H., “Design Evaluation and Use of a Reverberation Chamber for Performing Electromagnetic Susceptibility/Vulnerability Measurements,” NBS Technical Note 1092, Apr. 1986.

[B4] Freyer, G. J., and Hatfield, M. O., “Comparison of Gasket Transfer Impedance and Shielding Effectiveness Measurements,” *Proceedings of the 1992 IEEE International Symposium on Electromagnetic Compatibility,* Aug. 1992, pp. 139–148.

[B5] Freyer, G. J., Hatfield, M. O., Johnson, D. M., and Slocum, M. B., “Comparison of Measured and Theortical Parameters of Complex Cavities,” *Proceedings of the 1996 IEEE International Symposium on Electromagnetic Compatibility,* Aug. 1996.

[B6] Freyer, G. J., Rowan, J., and Hatfield, M. O., "Gasket Shielding Performance Measurements Obtained from Four Test Techniques," *Proceedings of the 1994 IEEE International Symposium on Electromagnetic Compatibility*, Aug. 1994, pp. 279–284.

[B7] Hatfield, M. O., "Shielding Effectiveness Measurements Using Mode-Stirred Chambers: A Comparison of Two Approaches," *IEEE Transactions on Electromagnetic Compatibility*, vol. 30, no. 3, Aug. 1988, pp. 229–238.

[B8] Jordan, E. C., *Electromagnetic Waves and Radiating Systems*. Englewood Cliffs, NJ: Prentice-Hall, Inc., 1950.

[B9] Kunkel, G. M., "Electromagnetic Leakage Through Slot Configurations in a Shielded Enclosure," *Proceedings of the 1994 IEEE International Symposium on Electromagnetic Compatibility*, 94CH3347-2, Aug. 1994, pp. 274–277.

[B10] Lehman, T. H., "A Statistical Theory of Electromagnetic Fields in Complex Cavities," *Interaction Notes*, Note 494, USAF Phillips Laboratory, May 1993.

[B11] Lehman, T. H., "Statistics of MSCs," *Anechoic Chamber and Reverberation Chamber Operator Users Group Meeting*, Naval Surface Warfare Center, Dahlgren, VA, Nov. 1992.

[B12] Marcuvitz, N., Editor, *Waveguide Handbook*. New York, NY: McGraw-Hill, 1951.

[B13] MIL-STD-285 (1956), Method of Attenuation Measurement for Enclosures, Electromagnetic Shielding, for Electronic Test Purposes.

[B14] NIS 81, The Treatment of Uncertainty in EMC Measurements.[9]

[B15] Peregrim, W. D., "Improved Radiated Test Method for Evaluating RF Shielding Gaskets and Material," *Proceedings of the 1993 IEEE International Symposium on Electromagnetic Compatibility*, Aug. 1993, pp. 241–244.

[B16] Quine, J. P., "Application of the Optical 'Black Hole' Principle to the Estimation of Shielding Effectiveness to Radio Frequency Energy," *Proceedings of the 1994 IEEE National Symposium on Electromagnetic Compatibility*, 89CH2736, May 1989, pp. 33–35.

[B17] Quine, J. P., "Characterization and Testing of Shielding Gasket at Microwave Frequencies," *Proceedings of the 1993 IEEE International Symposium on Electromagnetic Compatibility*, Aug. 1993, pp. 306–308.

[B18] Quine, J. P., et al., "Distortion of Radiation Patterns for Leakage Power Transmitted Through Attenuating Cover Panels and Shielding Gaskets—Need for Reverberation Chamber Measurements of Total Leakage Power," *Proceedings of the 1994 IEEE International Symposium on Electromagnetic Compatibility*, 94CH3347-2, Aug. 1994, pp. 285–290.

[B19] Quine, J. P., et al., "New and Simple Method for the Direct Measurement of Microwave Power Radiated from Gasketed Seams," *Proceedings of the 1996 IEEE International Symposium on Electromagnetic Compatibility*, Aug.1996, p. 391.

[B20] Quine, J. P., et al., "Proposal for a New Methodology Standard: Simple Near-Field Probe Measurements of Microwave Leakage Power from Gasketed Seams," *Proceedings of the 1997 IEEE International Symposium on Electromagnetic Compatibility*, 97CH36113, Aug. 1997, pp. 129–134.

[B21] Quine, J. P., and Pesta, A. J., "Shielding Effectiveness of an Enclosure Employing Gasketed Seams—Relation Between Shielding Enclosure and Gasket Transfer Impedance," *Proceedings of the 1995 IEEE International Symposium on Electromagnetic Compatibility*, Aug. 1995, pp. 392–395.

[B22] Schelkunoff, S. A., *Electromagnetic Waves*. New York, NY: Van Nostrand Co., Inc., 1943.

[9]Published by the National Physical Laboratory of the United Kingdom (FAX: 01181-943-7134).

To order IEEE standards…

Call 1. 800. 678. IEEE (4333) in the US and Canada.

Outside of the US and Canada:
1. 732. 981. 0600

To order by fax:
1. 732. 981. 9667

IEEE business hours: 8 a.m.–4:30 p.m. (EST)

For on-line access to IEEE standards information…

Via the World Wide Web:
http://standards.ieee.org/

Via ftp:
stdsbbs.ieee.org

**ISBN 0-7381-0183-4**